DOI: 10.1002/marc.((insert number)) ((or ppap., mabi., macp., mame., mren., mats.))

Article Type (Communication)

Facile Photochemical Modification of Silk Protein-Based Biomaterials[a]

John G. Hardy [1,2,3], Annabelle Bertin [4,5], Jose Guillermo Torres-Rendon [6], Aldo Leal-Egaña [1,7], Martin Humenik [1], Felix Bauer [1], Andreas Walther [6,8,9,10], Helmut Cölfen [11], Helmut Schlaad [12], and Thomas R. Scheibel [1,13,14,15,16,17,*]

[1] University of Bayreuth, Chair of Biomaterials, Universitätsstraße 30, 95447 Bayreuth, Germany
[2] Lancaster University, Department of Chemistry, Lancaster, LA1 4YB, UK
[3] Lancaster University, Materials Science Institute, Lancaster, LA1 4YB, UK
[4] German Federal Institute for Materials Research and Testing (BAM), Unter den Eichen 87, 12205 Berlin, Germany
[5] Free University of Berlin, Institute of Chemistry and Biochemistry, Takustraße 3, 14195 Berlin, Germany
[6] DWI Leibniz Institute for Interactive Materials, Forckenbeckstraße 50, 52056 Aachen, Germany
[7] University of Erlangen-Nuremberg, Institute of Biomaterials, Ulrich-Schalk-Straße 3, 91056 Erlangen, Germany
[8] University of Freiburg, Institute for Macromolecular Chemistry, Stefan-Meier-Straße 31, 79104 Freiburg, Germany
[9] University of Freiburg, Freiburg Materials Research Center, Stefan-Meier-Straße 21, 79104 Freiburg, Germany
[10] University of Freiburg, Freiburg Center for Interactive Materials and Bioinspired Technologies, Georges-Köhler-Allee 105, 79110 Freiburg, Germany
[11] University of Konstanz, Physical Chemistry, Department of Chemistry, Universitätsstraße 10, 78457 Konstanz, Germany
[12] University of Potsdam, Institute of Chemistry, Karl-Liebknecht-Straße 24-25, 14476 Potsdam, Germany
[13] Bayreuther Zentrum für Kolloide und Grenzflächen (BZKG), Universität Bayreuth, Universitätsstraße 30, 95440 Bayreuth, Germany
[14] Bayerisches Polymerinstitut (BPI), Universität Bayreuth, Universitätsstraße 30, 95440 Bayreuth, Germany
[15] Bayreuther Zentrum für Bio-Makromoleküle (bio-mac), Universität Bayreuth, Universitätsstraße 30, 95440 Bayreuth, Germany
[16] Bayreuther Zentrum für Molekulare Biowissenschaften (BZMB), Universität Bayreuth, Universitätsstraße 30, 95440 Bayreuth, Germany

[a] **Supporting Information** ((bold)) is available online from the Wiley Online Library or from the author.

[17] Bayreuther Materialzentrum (BayMAT), Universität Bayreuth, Universitätsstraße 30, 95440 Bayreuth, Germany

ABSTRACT

Silk protein-based materials show promise for application as biomaterials for tissue engineering. We report the simple and rapid photochemical modification of silk protein-based materials composed of either *Bombyx mori* silkworm silk or engineered spider silk proteins (eADF4(C16)). Radicals formed on the silk-based materials initiate the polymerization of monomers (acrylic acid, methacrylic acid, or allylamine) which functionalized the surface of the silk materials with poly(acrylic acid) (PAA), poly(methacrylic acid) (PMAA), or poly(allylamine) (PAAm). To demonstrate potential applications of this novel photochemistry we mineralized the polymer modified silks. The PAA and PMAA functionalized silks were mineralized with calcium carbonate, whereas the PAAm functionalized silks were mineralized with silica, both of which provide a coating on the materials that may be useful for bone tissue engineering, which will be the subject of future investigations.

FIGURE FOR ToC_ABSTRACT

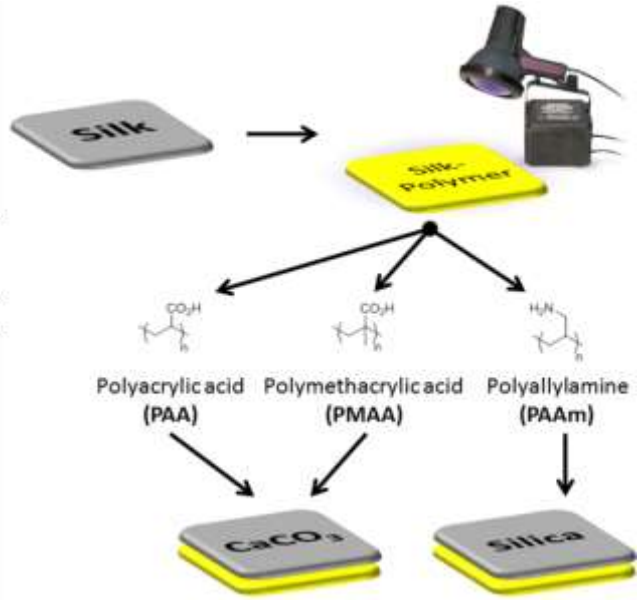
Silk
Silk-polymer
Polyacrylic acid
(PAA)
Polymethacrylic acid
(PMAA)
Polyallylamine
(PAAm)
CaCO3
Silica

1. Introduction

Silk-based materials are employed for a variety of technical applications (*e.g.*, textiles, optics, electronics) and medical applications (*e.g.*, sutures, drug delivery, tissue engineering).[1-3] Sources of such proteins include natural sources: domesticated *Bombyx mori* silkworms, bees, lacewings, and spiders (e.g. *Araneus diadematus*, *Nephila clavipes*),[1,4,5] as well as recombinantly produced engineered silk proteins that are a particularly attractive source of spider silk-mimetic proteins due to the inherent difficulty in farming spiders.[3,6,7] While the naturally produced silk of *B. mori* silkworms is currently the most economically important silk, industries are beginning to exploit engineered spider silks for commercial purposes. Silk proteins are processable in various solvents, which has enabled the production of diverse materials morphologies (e.g. films, fibers, foams, hydrogels and particulates) of use in both technical and biomedical industries.[8-10] The properties of such materials can be tuned to fit a specific application by either re-engineering the protein[3,6,7] or chemically as discussed previously.[11] Indeed, chemical modification of silkworm silks has been the subject of extensive research, historically focused on the textiles industry, and a popular route to chemically modify silk-based textiles is their exposure to initiators that generate radicals on the backbone of the silk protein enabling it to act as a macroinitiator to facilitate grafting of other polymers from their surface (modifying their finish, wettability etc.).[11] We and others have investigated the chemical modification of engineered spider silks (particularly of carboxylic acid and thiol moieties) to display cell adhesive peptides, polymers or nanoparticles which may impart novel functionality to the surface of the materials and improve their properties for application as tissue scaffolds.[1-3, 11]

Silk-based tissue scaffolds have been investigated for application in a variety of different biological niches,[1-3] including bone tissues which are hierarchically structured inorganic-

organic composite materials.[12] A variety of materials are under investigation to enhance bone regeneration (which is of great importance in societies with ageing populations),[13-15] one class of which include silk-based composite materials,[16] that may be mineralized[17-21] using a variety of approaches to yield scaffolds for bone regeneration.[22-26]

Protein-based materials are known to undergo photooxidation mediated by radical generation upon exposure to a high level of UV light.[27-31] UV-induced surface graft polymerizations using photoinitiators are a popular method of functionalizing a variety of surfaces.[32] Here we report the use of the silk proteins as initiators (when undergoing photooxidation mediated by radical generation upon exposure to a high level of UV light) to grow polymers from the backbone of *B. mori* silkworm silk fibroin (BMF) and engineered spider silks (eADF4(C16))[33] to display polymers. The polymers used to exemplify this approach were poly(acrylic acid) (PAA), poly(methacrylic acid) (PMAA) or poly(allylamine) (PAAm). Optionally, the polymers were mineralized with popular inorganic components of bone tissue scaffolds (specifically with calcium carbonate on PAA or PMAA modified silk, or silica on PAAm modified silk), and human mesenchymal stem cells were cultured on the materials in vitro.

2. Experimental Section

Full experimental details are found in the supplementary information.

3. Results and Discussion

The surface of silk protein-based biomaterials was modified using a simple photochemical approach wherein degummed BMF fibers[34] or films of eADF4(C16)[35] were immersed in neat monomer (acrylic acid, methacrylic acid or allylamine), exposed to UV light for 48 hours and subsequently washed and dried under vacuum. Exposure of the silk-based materials to high levels of UV light results in radical generation on the backbone of the silk proteins (which is

commonly known for proteins) and growth of polymers (PAA, PMAA or PAAm, respectively) grafted to the backbone of the silks (Figure 1).[36] SEM revealed clear differences between the surfaces of the unmodified and modified fibers (Figure 1), with the surfaces of the BMF fibers (Figure 1B) being relatively smooth by comparison with those modified with the materials when exposed to UV light in the absence (Figure 2C) or presence of monomers (Figure 2D to 2F), acrylic acid (Figure 2D), methacrylic acid (Figure 2E) or allylamine (Figure 2F), respectively. SEM (Figure S1) and water contact angle measurements (Table S1) for the eADF4(C16) films showed no statistically significant differences, however, modification of the surface chemistry of the films was confirmed by FTIR spectroscopy (Figure S2) and XPS (Figure 2).

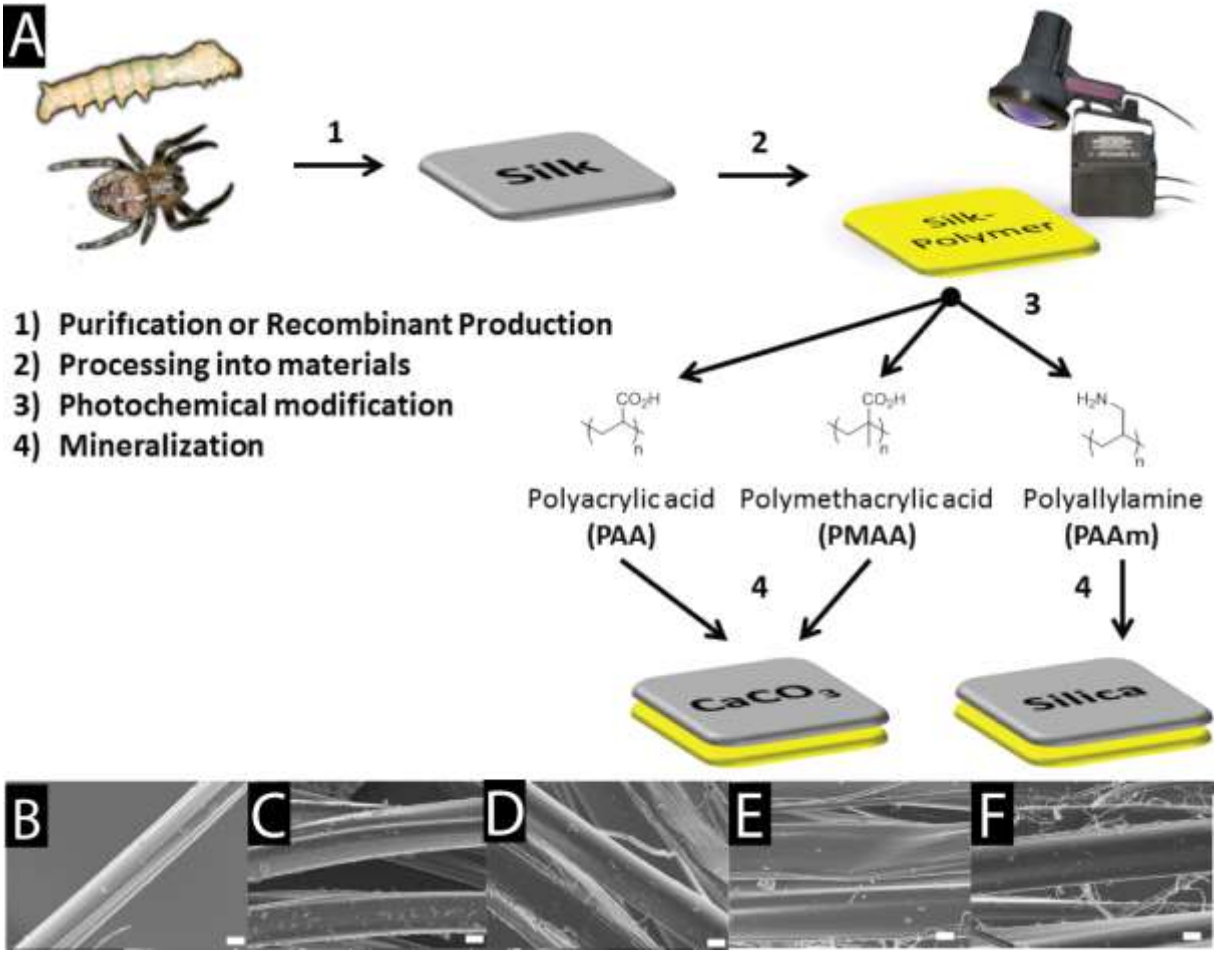

Figure 1. A) Schematic of the photochemical modification of silk-based materials with PAA, PMAA or PAAm and the optional mineralization of PAA-/PMAA-modified silks with calcium

carbonate, or of PAAm-modified silks with silica. B-F) SEM images of silk-based fibers, scale bars represent 4 µm. B) Degummed *B. mori* fibroin (BMF) fibers. C) Degummed BMF fibers exposed to UV light in the dry state. D) Degummed BMF fibers exposed to UV light in acrylic acid. E) Degummed BMF fibers exposed to UV light in methacrylic acid. F) Degummed BMF fibers exposed to UV light in allylamine.

Fourier transform infrared (FTIR) spectroscopy in attenuated total reflection (ATR) mode (Figure S2) revealed that the materials were all β-sheet rich, with peaks at 1620 (amide I), and 1520 cm^{-1} (amide II), for BMF fibers;[37,38] and 1624 cm^{-1} (amide I), 1520 cm^{-1} (amide II), and 964 cm^{-1} (polyalanine), for eADF4(C16) films.[33,35] Subtle qualitative changes in the spectra for BMF fibers and for films of eADF4(C16) modified with the monomers were observed. Indeed the materials with PAAm showed N-H bond bending vibrations being visible as a small shoulder at 1643 cm^{-1}, and the CH_2 bending vibration is visible as a small shoulder at 1444 cm^{-1},[39] with a notable diminishment of the COOH peak displayed on the backbone of eADF4(C16). The materials modified with PAA or PMAA showed minor alterations in peak intensity and breadth for the COOH peak at ca. 1700-1740 cm^{-1} confirming their presence. The fact that it is possible to observe peaks from the underlying protein suggests that the thickness of the layer of polymer on the surface of the films is on the nanometer scale as the IR beam on the ATR probe typically penetrates the top ca. 200 nm of the surface of the film.

XPS also confirmed the modification of the surface chemistry of the spin-coated eADF4(C16) films (Figure 2). XPS spectra of untreated spin-coated films of eADF4(C16) are displayed in Figure 2 A-C, those for films exposed to UV light in acrylic acid are displayed in Figure 2 D-F, those for films exposed to UV light in methacrylic acid are displayed in Figure 2 G-I, and those for films exposed to UV light in allylamine are displayed in Figure 2 J-L. The peak

shapes for the C 1s, O 1s and N 1s peaks showed significant differences for each of the different chemical modifications with PAA, PMAA and PAAm, respectively.

The C 1s peaks for the eADF4(C16) films (Figure 2A) showed significant changes as the variety of C 1s environments exposed on the surface of the films was diminished from carbons in the protein backbone and on the pendant side groups of the individual amino acids (e.g. C-C [alkyl and aromatic], C-H [alkyl and aromatic], C-N [in the backbone amides and on Glutamine], C=O [backbone amides and Glutamic acid], C-O [Glutamic acid, Serine, Tyrosine]) to those on PAA (Figure 2D), PMAA (Figure 2G) and PAAm (Figure 2J), *i.e.*, C-C [alkyl], C-H [alkyl], C-O and C=O [carboxylic acids on PAA and PMAA] and C-N [on PAAm]).

The O 1s peaks for the eADF4(C16) films (Figure 2B) showed minor changes for the PAA (Figure 2E), PMAA (Figure 2H) and PAAm (Figure 2K) modified films. The variety of O 1s environments exposed on the surface of the films is somewhat altered from oxygens in the protein backbone and on the pendant side groups of the individual amino acids (e.g. C=O [backbone amides and Glutamic acid], C-O and O-H [Glutamic acid, Serine, Tyrosine]), to C=O, C-O and O-H from the carboxylic acids on PAA and PMAA modified films). In agreement with the FTIR data this confirmed that the thickness of the coating of polymers is on the nanometer scale.

The N 1s peaks for the eADF4(C16) films (Figure 2C) showed clear changes for the films modified with PAA (Figure 2F), PMAA (Figure 2I) and PAAm (Figure 2L). The variety of N 1s environments exposed on the surface of the films was diminished from nitrogens in the protein backbone and on the pendant side groups of the individual amino acids (e.g. C-N and N-H in the backbone amides and on Glutamine), and the PAA and PMAA modified films had little/no nitrogen on the surface of the films, whereas the PAAm modified films had a clear N 1s peak because of the presence of C-N and N-H environments in the amines of PAAm.

Thereby the N 1s data showed that the coating of polymers on the surface of the films is homogeneous, akin to data from some of our previous work on the chemical modification of silk surfaces.[40]

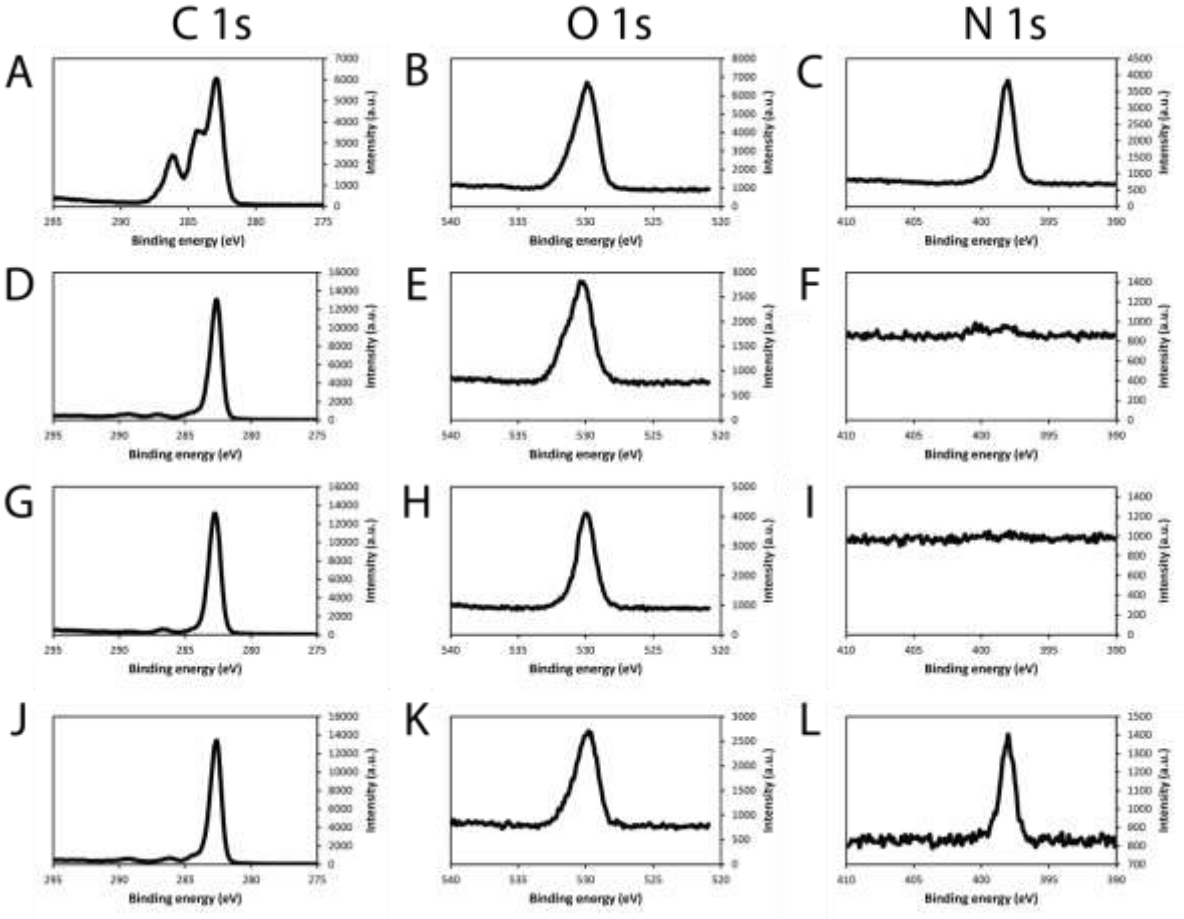

Figure 2. XPS analysis of spin-coated film of eADF4(C16), displaying the photoelectron spectra for C1s, O1s and N1s orbitals. A-C) Untreated. D-F) Exposed to UV light in acrylic acid. G-I) Exposed to UV light in methacrylic acid. J-L) Exposed to UV light in allylamine.

In addition to the SEM images and FTIR data that demonstrated the photochemical modification of the BMF fibers with PAA, PAAm and PMAA, data from TGA (Figure S3 and Table S2), DSC (Figure S4) and mechanical tests (Table S2) confirmed this. TGA profiles of degummed BMF fibers and the polymer modified fibers (Figure S3) were generally similar, however, the first derivatives of the TGA profiles revealed improvements in their thermal

stabilities (Table S2) after modification of the BMF fibers with PAA (+ ca. 7 °C), PAAm (+ ca. 15 °C) or PMAA (+ ca. 15 °C). DSC data showed subtle differences in the thermographs, with the thermal stabilities of the fibers showing a similar trend to the TGA data, increasing from the BMF fibers exposed to UV light, to the PAA modified fibers, then the PAAm modified fibers, and the most stable being PMAA modified fibers (Figure S4). The Young's moduli obtained from tensile testing (Table S2) showed some moderate improvements in the mechanical properties of BMF fibers modified with PAA and PMAA, although these differences were not statistically significant.

With a view to demonstrating potential applications of this photochemistry approach we mineralized the polymer modified silks. The carboxylic acid residues displayed on the proteins (C-terminus, aspartic acid, glutamic acid) and polymers (PAA and PMAA) can bind Ca^{2+} ions enabling the deposition of $CaCO_3$, which is of interest for biomedical applications e.g. in bone tissue regeneration.[25,41,42] SEM (Figure 3) revealed the deposition of $CaCO_3$ crystals on the surface of silk fibers and films. BMF fibers display few carboxylic acids and therefore deposition of $CaCO_3$ crystals was relatively low (Figure 3A), whereas those coated with PAA (Figure 3B) or PMAA (Figure 3C) were markedly more mineralized. The engineered spider silk eADF4(C16) displayed a higher proportion of carboxylic acids than BMF and therefore was more mineralized (Figure 3D), however, the films of eADF4(C16) coated with PAA (Figure 3E) or PMAA (Figure 3F) had a markedly increased density of carboxylic acids than the eADF4(C16) alone and were therefore the most highly mineralized substrates (also supporting the homogeneity of the polymer coatings on the silks).

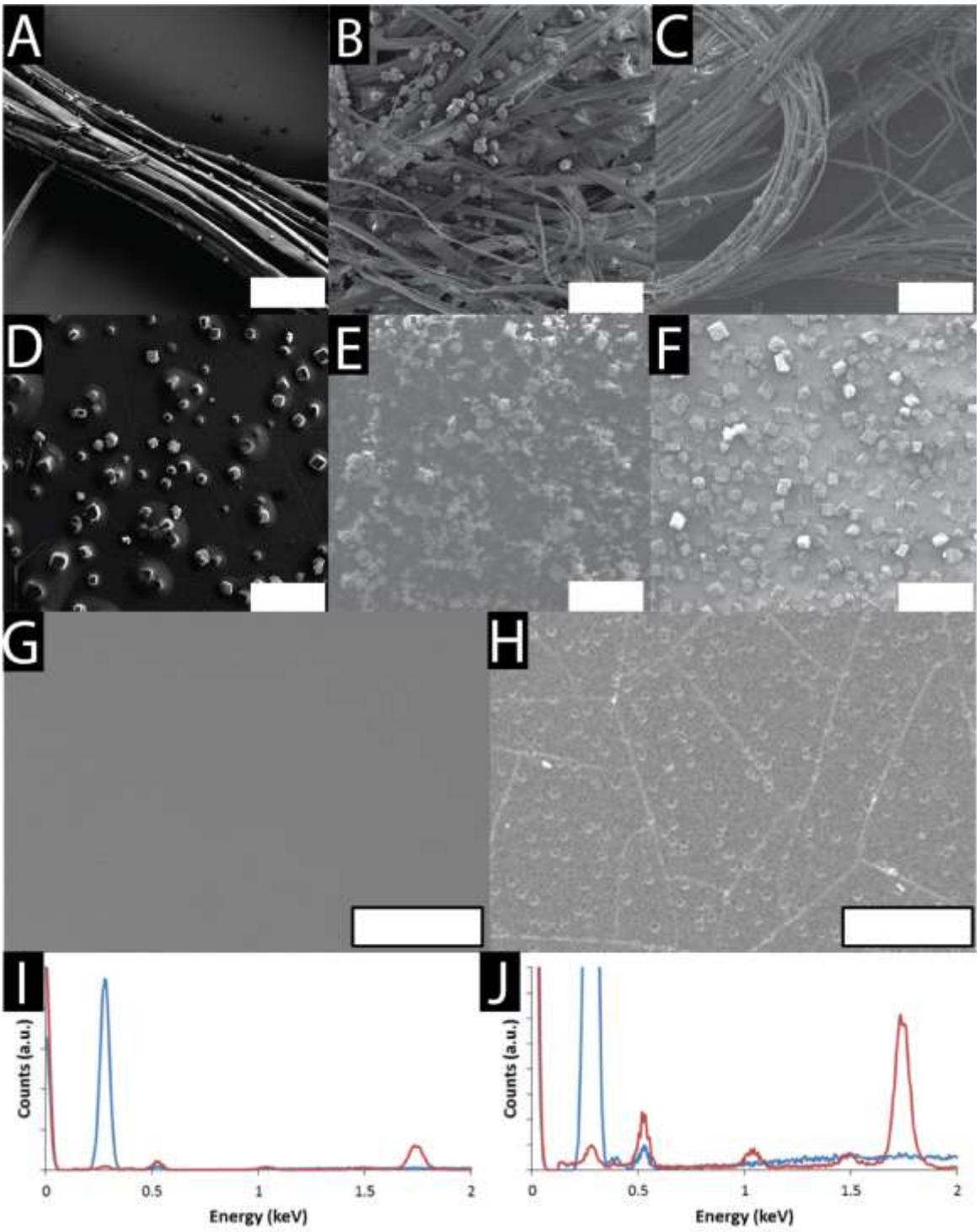

Figure 3. A-F) SEM images of silk-based materials after mineralization with $CaCO_3$, scale bars represent 200 µm. A) Mineralized unmodified BMF fibers. B) Mineralized PAA-coated BMF fibers. C) Mineralized PMAA-coated BMF fibers. D) Mineralized film of eADF4(C16). E) Mineralized PAA-coated film of eADF4(C16). F) Mineralized PMAA-coated film of eADF4(C16). G-J) SEM and EDS analysis of PAAm-modified silk-based materials, scale bars

represent 100 µm. G) SEM image of PAAm-modified film of eADF4(C16). H) SEM image of PAAm-modified film of eADF4(C16) mineralized with silica. I) EDS analysis of PAAm-modified films of eADF4(C16) before (blue) and after (red) mineralization with silica. J) Enlarged version of I.

The amines displayed on the PAAm modified engineered spider silk eADF4(C16) facilitated the deposition of silica, which is also of interest for the aforementioned biomedical applications.[22,23] SEM and Energy dispersive X-ray (EDS) analysis of the films before and after mineralization with silica showed clear differences. The SEM images showed the smooth surface of the films before mineralization with silica (Figure 3G), and that after mineralization with silica (Figure 3H) there was a layer of silica with nanometer to micrometer scale pores present on the surface. EDS confirmed that their surface chemistry was different before and after mineralization (Figure 3I and 3J). Peaks in the EDS spectra of the films of PAAm modified eADF4(C16) had lines at 0.277 and 0.525 keV that are the characteristic Kα emissions of carbon and oxygen (Figure 3I), respectively, and the very weak emission at 0.392 keV is the Kα emission of nitrogen (clearest in Figure 3J). The peak at 1.041 keV is the Kα emission of sodium from the phosphate buffered saline used in the mineralization process (Figure 3I and 3J). The peak at 1.480 keV is the Kα emission of bromine and is plausibly because of traces of bromine impurities in the salt used during buffer preparation for use in the mineralization process (Figure 3I and 3J). Importantly, the successful mineralization of the films of PAAm modified eADF4(C16) with silica was clear from the appearance of the Kα emission peak of silicon at 1.739 keV (Figure 3I and 3J).
To demonstrate biocompatibility, human mesenchymal stem cells were cultured in vitro for 2 weeks on the materials. Alkaline phosphatase (ALP) activity is a hallmark of bone tissue formation, and qualitative analysis of ALP activity was demonstrated with ALP live staining

(Figure S5) which showed that the cells were alive and functional (on or indeed infiltrated inside the films) as seen by the patches of dark coloration that is characteristic of the precipitated stain. As previously reported, cells adhere better on Nunclon® Δ tissue culture plastic (Figure S5A) than on eADF4(C16) which is clearly evident here (Figure S5B). The opacity of the calcium carbonate mineralized films on PAA modified eADF4(C16) (Figure S5C), or on PMAA modified eADF4(C16)) (Figure S5D) rendered microscopy challenging, as did the porosity of the silica coating on the PAAm modified eADF4(C16) (Figure S5E) where cells appeared to have infiltrated the pores. The evidence of ALP activity on such materials suggested that they are worthy of further investigation into their potential for bone tissue engineering, particularly in light of studies of MC3T3 cells grown on $CaCO_3$ scaffolds which exhibited markedly increased ALP activity, higher levels of growth factors which regulate osteoblast differentiation, and matrix mineralization (calcium deposition), all of which are important biomarkers for bone tissue formation.[43] Such results demonstrate the potential benefit of employing $CaCO_3$ scaffolds for bone tissue engineering applications.[44-47]

4. Conclusions

Silk protein-based materials are being developed for a wide variety of technical and biomedical applications.[48,49] We report the simple modification of silk protein-based materials composed of either degummed *B. mori* fibroin or an engineered spider silk protein (eADF4(C16)) with polymers (PAA, PMAA or PAAm). Furthermore, we demonstrated potential applications of this novel photochemistry by mineralization of the polymer modified silks: the PAA and PMAA functionalized silks were mineralized with calcium carbonate, whereas the PAAm functionalized silks were mineralized with silica, both of which provide a coating on the materials that may be useful for bone tissue engineering as exemplified by cell culture studies in vitro. We conclude that the simple photochemical

modification of silk protein-based materials reported in this manuscript should be useful for a variety of applications,[50] including the development of functional mineralized biomaterials for regenerative medicine.

Supporting Information

Supporting Information is available from the Wiley Online Library or from the author.

Acknowledgements:

We thank the Alexander von Humboldt Foundation for a postdoctoral fellowship for J.G.H, and the German Research Foundation (Deutsche Forschungsgemeinschaft, SFB 840 TP A8) for financial support for T.R.S. At the University of Bayreuth we thank Andreas Schmidt and Johannes Diehl for assistance with protein production and purification; we thank Markus Hecht and Laura Kloth for assistance with sample preparation; we thank Hendrik Bargel for assistance with SEM; we thank Alexandra Witt and Ute Kuhn for assistance with DSC and TGA; we thank Markus Hecht and Reiner Giesa for assistance with tensile testing, and Markus Hecht and Elke Fuchs for assistance with contact angle measurements.

Received: Month XX, XXXX; Revised: Month XX, XXXX; Published online:

((For PPP, use "Accepted: Month XX, XXXX" instead of "Published online")); DOI: 10.1002/marc.((insert number)) ((or ppap., mabi., macp., mame., mren., mats.))

Keywords: silkworm silk, spider silk, chemical modification, photochemistry, biomaterials

[1.] Jao, D.; Mou, X.; Hu, X. Tissue Regeneration: A Silk Road. *J. Funct. Biomater*. **2016**, *7* (3), 22.

[2.] Altman, G. H.; Diaz, F.; Jakuba, C.; Calabro, T.; Horan, R. L.; Chen, J.; Lu, H.; Richmond, J.; Kaplan, D.L. Silk-based biomaterials. *Biomaterials*. **2003**, *24* (3), 401-16.

[3.] Aigner, T. B.; DeSimone, E.; Scheibel, T. Biomedical Applications of Recombinant Silk-Based Materials. *Adv. Mater*. **2018**, *30* (19), 1704640.

[4.] Sutherland, T. D.; Young, J. H.; Weisman, S.; Hayashi, C. Y.; Merritt, D. J. Insect silk: one name, many materials. Annu. Rev. Entomol. **2010**, *55*, 171-188.

[5.] Craig, C. L.; Hsu, M.; Kaplan, D.; Pierce, N. E. A comparison of the composition of silk proteins produced by spiders and insects. *Int. J. Biol. Macromol*. **1999**, *24* (2-3), 109-118.

[6.] Sutherland, T. D.; Rapson, T. D.; Huson, M. G.; Church, J. S. Recombinant Structural Proteins and Their Use in Future Materials. *Subcell. Biochem*. **2017**, *82*, 491-526.

[7.] Dinjaski, N.; Kaplan, D. L. Recombinant protein blends: silk beyond natural design. *Curr. Opin. Biotechnol*. **2015**, *39*, 1-7.

[8.] Koeppel, A.; Holland, C. Progress and Trends in Artificial Silk Spinning: A Systematic Review. *ACS Biomater. Sci. Eng.*, **2017**, *3* (3), 226–237.

[9.] Hardy, J. G.; Scheibel, T. R. Production and processing of spider silk proteins. *J. Polym. Sci. Part A: Polym. Chem.* **2009**, *47* (16), 3957-3963.

[10.] Schacht, K; Scheibel, T. Processing of recombinant spider silk proteins into tailor-made materials for biomaterials applications. *Curr. Opin. Biotechnol*. **2014**, *29*, 62-69.

[11.] Murphy, A. R.; Kaplan, D. L. Biomedical applications of chemically-modified silk fibroin. *J. Mater. Chem*. **2009**, *19* (36), 6443-6450.

[12.] Olszta, M. J.; Cheng, X. G.; Jee, S. S.; Kumar, R.; Kim, Y. Y.; Kaufman, M. J.; Douglas, E. P.; Gower, L. B. Bone structure and formation: A new perspective. *Mater. Sci. Eng. R-Reports* **2007**, *58*, 77-116.

[13.] Raucci, M. G.; Guarino, V.; Ambrosio, L. Biomimetic Strategies for Bone Repair and Regeneration. *J. Funct. Biomater*. **2012**, *3* (3), 688-705.

[14.] Gao, C.; Deng, Y.; Feng, P.; Mao, Z.; Li, P.; Yang, B.; Deng, J.; Cao, Y.; Shuai, C.; Peng, S. Current Progress in Bioactive Ceramic Scaffolds for Bone Repair and Regeneration. *Int. J. Mol. Sci.* **2014**, *15* (3), 4714-4732.

[15.] Fitzpatrick, L. E.; McDevitt, T. C. Cell-derived matrices for tissue engineering and regenerative medicine applications. *Biomater. Sci*. **2015**, *3*, 12-24.

[16.] Hardy, J. G.; Scheibel, T. R. Composite materials based on silk proteins. *Prog. Polym. Sci.* **2010**, *35* (9), 1093-1115.

[17.] Meldrum, F. C.; Cölfen, H. Controlling Mineral Morphologies and Structures in Biological and Synthetic Systems. *Chem. Rev.* **2008**, *108* (11), 4332-4432.

[18.] Gower, L. B. Biomimetic model systems for investigating the amorphous precursor pathway and its role in biomineralization. *Chem. Rev*. **2008**, *108* (11), 4551-4627.

[19.] Xu A.-W.; Ma, Y.; Cölfen, H. Biomimetic mineralization. *J. Mater. Chem*. **2007**, *17* (5), 415-449.

[20.] Sonnenberg, L.; Luo, Y.; Schlaad, H.; Seitz, M.; Cölfen, H.; Gaub, H. E. Quantitative single molecule measurements on the interaction forces of poly(L-glutamic acid) with calcite crystals. *J. Am. Chem. Soc*. **2007**, *129* (49), 15364-15371.

[21.] Casse, O.; Shkilnyy, A.; Linders, J.; Mayer, C.; Haussinger, D.; Völkel, A.; Thünemann, A. F.; Dimova, R.; Cölfen, H.; Meier, W.; Schlaad, H.; Taubert, A. Solution Behavior of

Double-Hydrophilic Block Copolymers in Dilute Aqueous Solution. *Macromolecules* **2012**, *45* (11), 4772-4777.

[22.] Wong Po Foo, C.; Patwardhan, S. V.; Belton, D. J.; Kitchel, B.; Anastasiades, D.; Huang, J.; Naik, R. R.; Perry, C. C.; Kaplan, D. L. Novel nanocomposites from spider silk-silica fusion (chimeric) proteins. *Proc. Natl. Acad. Sci. USA*. **2006**, *103* (25), 9428-9433.

[23.] Mieszawska, A. J.; Nadkarni, L. D.; Perry, C. C.; Kaplan, D. L. Nanoscale control of silica particle formation via silk-silica fusion proteins for bone regeneration. *Chem. Mater*. **2010**, *22* (20), 5780-5785.

[24.] Huang, X.; Liu, X.; Liu, S.; Zhang, A.; Lu, Q.; Kaplan, D. L.; Zhu, H. Biomineralization regulation by nano-sized features in silk fibroin proteins: synthesis of water-dispersible nano-hydroxyapatite. *J. Biomed. Mater. Res. B. Appl. Biomater.* **2014**, *102* (8), 1720-1729.

[25.] Zhang, X.; Fan, Z.; Lu, Q.; Huang, Y.; Kaplan, D. L.; Zhu, H. Hierarchical biomineralization of calcium carbonate regulated by silk microspheres. *Acta Biomater*. **2013**, *9* (6), 6974-6980.

[26.] Hardy, J. G.; Torres-Rendon, J. G.; Leal-Egaña, A.; Walther, A.; Schlaad, H.; Cölfen, H.; Scheibel, T. R. Biomineralization of Engineered Spider Silk Protein-Based Composite Materials for Bone Tissue Engineering. *Materials* **2016**, *9* (7), 560.

[27.] Egerton, G. S.; Some Aspects of the Photochemical Degradation of Nylon, Silk, and Viscose Rayon. *Text. Res. J.* **1948**, *18* (11), 659-669.

[28.] Baltova, S.; Vassileva, V.; Valtcheva, E. Photochemical behaviour of natural silk—I. Kinetic investigation of photoyellowing. *Polym. Degrad. Stab*. **1998**, *60* (1), 53-60.

[29.] Baltova, S.; Vassileva, V. Photochemical behaviour of natural silk—II. Mechanism of fibroin photodestruction. *Polym. Degrad. Stab*. **1998**, *60* (1), 61-65.

[30.] Shao, J.; Zheng, J.; Liu, J.; Carr, C. M. Fourier transform Raman and Fourier transform infrared spectroscopy studies of silk fibroin. *J. Appl. Polym. Sci*. **2005**, *96* (6), 1999-2004.

[31.] Lai, W. L.; Goh, K. L. Consequences of Ultra-Violet Irradiation on the Mechanical Properties of Spider Silk. J. Funct. Biomater. **2015**, *6* (3), 901-916.

[32.] Deng, J.; Wang, L.; Liu, L.; Yang, W. Developments and new applications of UV-induced surface graft polymerizations. *Prog. Polym. Sci*., **2009**, *34* (2), 156-193.

[33.] Huemmerich, D.; Helsen, C.W.; Quedzuweit, S.; Oschmann, J.; Rudolph, R.; Scheibel, T. Primary structure elements of spider dragline silks and their contribution to protein solubility. *Biochemistry* **2004**, *43* (42), 13604-13612.

[34.] Rockwood, D. N.; Preda, R. C.; Yücel, T.; Wang, X.; Lovett, M. L.; Kaplan, D. L. Materials fabrication from Bombyx mori silk fibroin. *Nat. Protoc*. **2011**, *6* (10), 1612-1631.

[35.] Junghans, F.; Morawietz, M.; Conrad, U.; Scheibel, T.; Heilmann, A.; Spohn, U. Preparation and mechanical properties of layers made of recombinant spider silk proteins and silk from silk worm. *Applied Physics A*, **2006**, *82* (2), 253–260.

[36.] Bertin, A.; Schlaad, H. Mild and Versatile (Bio-)Functionalization of Glass Surfaces via Thiol−Ene Photochemistry. *Chem. Mater.* **2009**, *21* (24), 5698–5700.

[37.] Ling, S.; Qi, Z.; Knight, D. P.; Shao, Z.; Chen, X. Synchrotron FTIR Microspectroscopy of Single Natural Silk Fibers. *Biomacromolecules* **2011**, *12* (9), 3344–3349.

[38.] Boulet-Audet, M.; Vollrath, F.; Holland, C. Identification and classification of silks using infrared spectroscopy. *J. Exp. Biol*. **2015**, *218* (19): 3138–3149.

[39.] Hu, J.; He, B.; Lu, J.; Hong, L.; Yuan, J.; Song, J.; Niu, L. Facile Preparation of Pt/Polyallylamine/Reduced Graphene Oxide Composites and Their Application in the

Electrochemical Catalysis on Methanol Oxidation, *Int. J. Electrochem. Sci*. **2012**, *7*, 10094-10107.

[40.] Hardy, J. G.; Leal-Egaña, A.; Scheibel, T. R. Engineered spider silk protein-based composites for drug delivery. *Macromol. Biosci*. **2013**, *13* (10), 1431-1437.

[41.] Woldetsadik, A. D.; Sharma, S. K.; Khapli, S.; Jagannathan, R., Magzoub, M. Hierarchically Porous Calcium Carbonate Scaffolds for Bone Tissue Engineering, *ACS Biomater. Sci. Eng*. **2017**, *3* (10), 2457–2469.

[42.] Astachov, L.; Nevo, Z.; Vago, R. Calcite Biohybrids as Microenvironment for Stem Cells. *Polymers* **2012**, *4* (2), 1065-1083.

[43.] Woldetsadik, A. D.; Sharma, S. K.; Khapli, S.; Jagannathan, R.; Magzoub, M. Hierarchically Porous Calcium Carbonate Scaffolds for Bone Tissue Engineering. *ACS Biomater. Sci. Eng*., **2017**, 3 (10), 2457–2469.

[44.] Astachov L, Nevo Z, Aviv M, Vago R. Crystalline calcium carbonate and hydrogels as microenvironment for stem cells. *Front Biosci (Landmark Ed).* **2011**, 16, 458-71.

[45.] Kharlampieva, E.; Kozlovskaya, V.; Gunawidjaja, R.; Shevchenko, V. V.; Vaia, R.; Naik, R. R.; Kaplan, D. L.; Tsukruk, V. V. Flexible Silk–Inorganic Nanocomposites: From Transparent to Highly Reflective. Adv. Funct. Mater., 2010, 20 (5), 840-846.

[46.] Kharlampieva, E.; Kozlovskaya, V.; Wallet, B.; Shevchenko, V.V.; Naik, R.R.; Vaia, R.; Kaplan, D.L.; Tsukruk, V.V. Co-cross-linking silk matrices with silica nanostructures for robust ultrathin nanocomposites. ACS Nano. 2010, 4 (12), 7053-63.

[47.] Grant, A. M., Kim, H. S.; Dupnock, T. L.; Hu, K.; Yingling, Y. G.; Tsukruk, V.V. Silk Fibroin–Substrate Interactions at Heterogeneous Nanocomposite Interfaces. Adv. Funct. Mater. 2016, 26 (35), 6380-6392.

[48.] Humenik, M.; Smith, A. M.; Scheibel, T. Recombinant Spider Silks—Biopolymers with Potential for Future Applications. *Polymers* **2011**, *3* (1), 640-661.

[49.] Widhe, M.; Johansson, J.; Hedhammar, M.; Rising, A. Invited review current progress and limitations of spider silk for biomedical applications. *Biopolymers* **2012**, *97* (6), 468-478.

[50.] Wang, G.; Zreiqat, H. Functional Coatings or Films for Hard-Tissue Applications. *Materials* **2010,** *3* (7), 3994-4050.

Simple and rapid photochemical modification of silk protein-based materials initiate the polymerization of monomers (acrylic acid, methacrylic acid, or allylamine) in order to functionalize the surface of silk materials.The functionalized silks were mineralized with calcium carbonate or silica, both of which provide a coating on the materials that may be useful for bone tissue engineering.

ToC figure

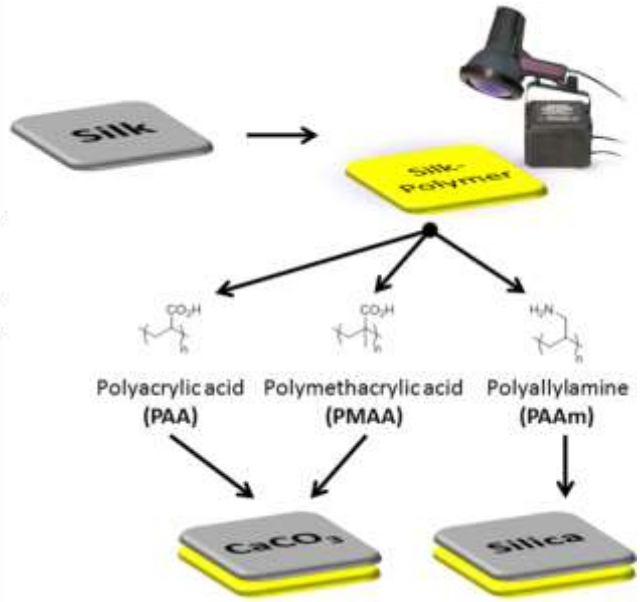

Captions to Figures/Schemes.

Figure 1. A) Schematic of the photochemical modification of silk-based materials with PAA, PMAA or PAAm and the optional mineralization of PAA-/PMAA-modified silks with calcium carbonate, or of PAAm-modified silks with silica. B-F) SEM images of silk-based fibers, scale bars represent 4 µm. B) Degummed *B. mori* fibroin (BMF) fibers. C) Degummed BMF fibers exposed to UV light in the dry state. D) Degummed BMF fibers exposed to UV light in acrylic acid. E) Degummed BMF fibers exposed to UV light in methacrylic acid. F) Degummed BMF fibers exposed to UV light in allylamine.

Figure 2. XPS analysis of spin-coated film of eADF4(C16), displaying the photoelectron spectra for C1s, O1s and N1s orbitals. A-C) Untreated. D-F) Exposed to UV light in acrylic acid. G-I) Exposed to UV light in methacrylic acid. J-L) Exposed to UV light in allylamine.

Figure 3. A-F) SEM images of silk-based materials after mineralization with $CaCO_3$, scale bars represent 200 µm. A) Mineralized unmodified BMF fibers. B) Mineralized PAA-coated BMF fibers. C) Mineralized PMAA-coated BMF fibers. D) Mineralized film of eADF4(C16). E) Mineralized PAA-coated film of eADF4(C16). F) Mineralized PMAA-coated film of eADF4(C16). G-J) SEM and EDS analysis of PAAm-modified silk-based materials, scale bars represent 100 µm. G) SEM image of PAAm-modified film of eADF4(C16). H) SEM image of PAAm-modified film of eADF4(C16) mineralized with silica. I) EDS analysis of PAAm-modified films of eADF4(C16) before (blue) and after (red) mineralization with silica. J) Enlarged version of I.